

## Low-temperature absorption and resonance Raman spectra of the $\text{MnO}_4^-$ ion doped in a $\text{KClO}_4$ crystal

M. Leuchs and W. Kiefer\*

*Institut für Physikalische Chemie der Universität Würzburg, Marcusstrasse 9-11  
97070 Würzburg, Federal Republic of Germany*

(Received 30 April 1993)

We have performed polarized absorption and resonance Raman experiments on a permanganate ion doped in a potassium perchlorate single crystal at temperature  $T = 15$  K. At this low temperature the  $m(C_s)$  site splitting of the excited degenerate  ${}^1T_2$  electronic level of the permanganate ion is well resolved and the amount of splitting is about  $40\text{ cm}^{-1}$ . Due to the electronic configuration, one would expect that non-Condon terms have to be considered in the description of the absorption spectrum. For the theoretical simulation of our experimental results we have used expressions derived from the time-correlator formulation for the optical absorption. These are much easier to handle and they cause significant shorter calculation times than the usual sum-over-states expressions. In order to determine the symmetries and the wave-number positions of the site-split permanganate vibrations, we have performed resonance Raman experiments. The results obtained from these experiments form the basis for the interpretation of the absorption spectrum. The applied model includes the linear and quadratic electron-phonon and linear non-Condon coupling. Within this model we describe the multimode system and we show how a normal vibration, which apparently has no significant effects in the absorption spectrum, influences the discussion of the model system. For the fully symmetric breathing mode of the permanganate ion, we have calculated the change of the Mn-O equilibrium bond length in the electronic excited state from the corresponding linear electron-phonon coupling constant to be  $4.6 \pm 0.4$  pm.

### I. INTRODUCTION

The permanganate ion can be regarded as a model system with respect to its vibronic structure because its low-temperature absorption and resonance Raman spectra allow one to derive detailed information concerning this structure. In the present paper we show how to calculate the polarized absorption spectrum by making use of resonance Raman data. The model applied is based on the time-correlator formulation for the optical absorption developed by Page and co-workers.<sup>1-9</sup> These authors have derived nonperturbative and numerically tractable results, which are applicable for a wide class of systems including electron-phonon interaction and non-Condon coupling.

Within this model the electron-phonon interaction arises from the change of the arbitrary harmonic vibrational Hamiltonian under electronic excitation, whereby the normal coordinates of the vibrational Hamiltonian in the electronic ground state are the natural variables in terms of which the model is parametrized. As the potential surfaces are allowed to be general harmonic, the operator of the electron-phonon ( $e$ -ph) interaction can be expressed in a power series up to the second order of the rescaled normal coordinates. The coefficients of the linear and quadratic terms define the linear and quadratic  $e$ -ph coupling coefficients. The non-Condon coupling arises from the dependence of the atomic configuration of the electronic transition dipole matrix element and in the most general model this dependence is again expressed as a power series up to the second order of the ground-state

rescaled normal coordinates. Corresponding to the  $e$ -ph interaction linear and quadratic non-Condon coefficients are defined by the coefficients of the power series. In our discussion we include only linear non-Condon terms.

Combined with the time-correlator formulation of the resonance Raman cross section, this theory gives a very useful connection between resonance Raman excitation profiles and the optical absorption spectrum, which is known as the transform theory.<sup>9</sup>

### II. RESONANCE RAMAN SPECTRA

In order to derive a theoretical absorption spectrum of the permanganate ion doped in potassium perchlorate, we first performed Raman experiments to determine the positions and the symmetries of the permanganate vibrations as well as low-frequency lattice modes. These modes will be needed later for the simulation of the absorption spectrum.

The mixed crystals were drawn from a nearly saturated potassium perchlorate solution with 0.5 wt. % of potassium permanganate.<sup>10</sup> Both components are isomorphic and have similar lattice constants; therefore, the perchlorate ions should be statistically substituted by the corresponding permanganate ions. Owing to the low concentration, the permanganate ions were regarded as non-self-interacting impurity centers. The symmetry of the free ions is changed to the site symmetry  $m(C_s)$  when the permanganate ions are incorporated in the host lattice. The relevant correlation splitting is shown in Table I. All irreducible representations of the site group and the fac-

TABLE I. Site group splitting of the free  $\text{MnO}_4^-$  ion. Additionally the factor group correlation is listed for the four  $\text{ClO}_4^-$  ions in the unit cell.

Free ion	$\text{MnO}_4^-$ ion Site group	$\text{ClO}_4^-$ ions Factor group
$43m(T_d)$	$m(C_s)$	$mmm(D_{2h})$
$(\nu_1)A_1$	$A'$	$A_g + B_{2g} + B_{1u} + B_{3u}$
$(\nu_2)E$	$A''$	$A_g + B_{2g} + B_{1u} + B_{3u}$
	$A''$	$B_{1g} + B_{3g} + A_u + B_{2u}$
$(\nu_3, \nu_4)T_2$	$2A'$	$2(A_g + B_{2g} + B_{1u} + B_{3u})$
	$A''$	$B_{1g} + B_{3g} + A_u + B_{2u}$

tor group are one dimensional and therefore the degeneration of all vibrations is removed. The mixed crystals used in our experiments<sup>10</sup> have been of small size only. Because of that, it was not possible to prepare special crystal surfaces and hence we could perform only two different polarization measurements. In the first experiment we choose the E vector parallel to the x axis, indicated by an index x, and in a second one we have used a polarization with components along the y and z axis, which is indicated by an index s. Figure 1 shows the Raman spectrum around the region of the breathing mode of the permanganate ion at  $850.8 \text{ cm}^{-1}$  as well as around the corresponding nonresonant perchlorate internal vibration at a wave-number position of  $944.8 \text{ cm}^{-1}$ . The latter band can be used as an internal standard for resonance Raman or resonance coherent anti-Stokes Raman spectroscopy (CARS) experiments.<sup>10,11</sup>

In the lower spectrum of Fig. 1 (indicated by  $|\alpha_{xs}|^2$ ) one can recognize the site splitted  $\nu_3$  permanganate vibration around  $915$  to  $945 \text{ cm}^{-1}$ . In the latter polarization

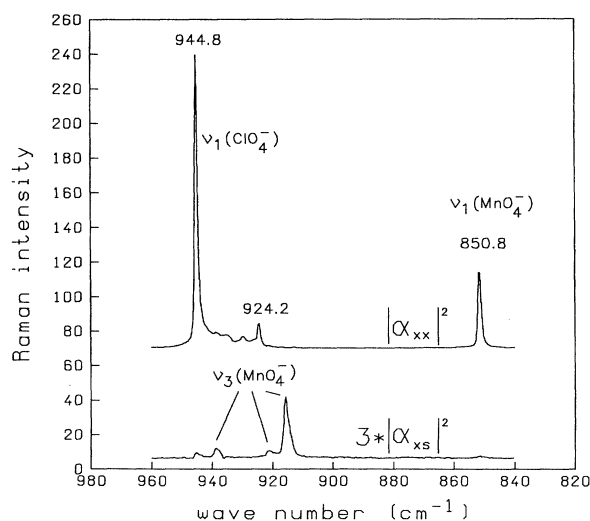


FIG. 1. Polarized resonance Raman spectra of  $\text{KClO}_4$  single-crystal doped with  $\text{MnO}_4^-$  ions at  $T=15 \text{ K}$ . To show more details, the intensity of the  $|\alpha_{xs}|^2$  spectrum was multiplied by a factor of 3. Excitation wavelength  $\lambda_0=514.5 \text{ nm}$  ( $19435 \text{ cm}^{-1}$ ).

spectrum both the  $A'$  and the  $A''$  modes are symmetry allowed (see Table II). Therefore, we cannot derive any more information on the symmetry of the corresponding normal vibrations from this spectrum. The site splitted  $\nu_4$  and  $\nu_2$  permanganate vibrations appear in the Raman spectra as fundamental, overtone, and combination bands. They are shown in more detail in Fig. 2. The wave-number positions of the fundamental vibrations can be directly extracted from  $|\alpha_{xx}|^2$ ,  $|\alpha_{xs}|^2$ , and the  $|\alpha_{ss}|^2$  spectra. For the split  $\nu_4$  and  $\nu_2$  modes we obtain wave number values of  $393.4$ ,  $396.0$ , and  $406.4 \text{ cm}^{-1}$  and  $354.2$  and  $360.3 \text{ cm}^{-1}$ , respectively. By making use of these values we have calculated combination and overtone bands of these fundamentals and we have listed them in Table III. The actual symmetry of the fundamentals is derived by a more detailed inspection of the selection rules, which follows next.

The Raman cross section<sup>12</sup>  $\sigma_R$  is proportional to  $\hat{e}_s \alpha^{(1)} \hat{e}_i$ , where  $\hat{e}_s$  and  $\hat{e}_i$  are the unit vectors of the polarization of the scattered and incident light, respectively. According to the applied scattering geometry<sup>10</sup> the selection rules for the linear Raman process as listed in Table II are valid. Thus, the Raman lines recorded in the  $|\alpha_{xx}|^2$  spectrum are of  $A'$  symmetry. The Raman line at  $396.0 \text{ cm}^{-1}$  has therefore  $A'$  symmetry. Since all vibrations are nondegenerate the symmetry discussion for combination and overtone vibrations is straightforward.<sup>13</sup> In principle, the symmetry of combination of fundamental vibrations is given by the direct product of the representations of the fundamental vibrations. As an example, the combination of one  $A'$  and one  $A''$  normal vibration has  $A''$  symmetry. The even overtone levels ( $\nu_k=2,4,\dots$ ; with  $\nu_k$  being the quantum number of the  $k$ th normal mode) of nondegenerate normal vibrations belong to the totally symmetric representation  $A'$ . Using these results the symmetry of the fundamentals can easily be determined. The result of the classification of the site splitted  $\nu_4$  and  $\nu_2$  vibrations is listed in Table IV.

As has been reported in Ref. 14 the vibrational structure of the absorption spectrum contains an additional low-frequency lattice mode. To confirm this observation, we have recorded Raman spectra of the mixed as well as of the host crystal. They are displayed in Fig. 3. Comparing spectra 3(a) and 3(b) and 3(c) and 3(d), respectively, one can distinguish between nonlocalized Raman lines<sup>15</sup> of the pure host lattice and the localized ones due to six external degrees of freedom corresponding to the site split translational ( $T_2 \rightarrow 2A' + A''$ ) and rotational ( $T_1 \rightarrow A' + 2A''$ ) motions of the impurity in its surrounding cage. These additional permanganate Raman lines are marked with an asterisk in spectra 3(b) and 3(d) displayed in Fig. 3. Since the Raman lines<sup>10</sup> of the pure host lattice show no significant difference when compared with the Raman lines of the host lattice in the mixed crystals, the breakdown of the translatory symmetry caused by the impurity ions is therefore neglected in our discussion of the Raman spectra. We have confirmed these results by additional Raman spectra which are not reproduced in the present paper.

The correct determination of the internal vibrational frequencies and the symmetries of the permanganate vi-

TABLE II. Selection rules for the different kinds of the scattering geometries.  $\hat{e}_i$  unit vector of the polarization of the incident light,  $\hat{e}_s$  unit vector of the polarization of the scattered light. Used abbreviations: sg=site group and fg=factor group.

$\hat{e}_s$	$\hat{e}_i$	Tensor components	Irred. rep. <sub>sg</sub>	Irred. Rep. <sub>fg</sub>
(1,0,0)	(1,0,0)	$xx \rightarrow  \alpha_{xx} ^2$	$A'$	$A_g$
(1,0,0)	(0,a,b)	$xz, xy \rightarrow  \alpha_{xs} ^2$	$A', A''$	$B_{2g}, B_{1g}$
(0,a,b)	(0,a,b)	$yy, zz, zy, yz \rightarrow  \alpha_{ss} ^2$	$A', A''$	$A_g, B_{3g}$

brations as well as of the lattice modes in the electronic ground state of the system is necessary for a theoretical simulation of the absorption spectrum, which is given next.

### III. THEORY FOR SIMULATION OF THE ABSORPTION SPECTRUM

In the basic model<sup>9</sup> the electronic states are localized and a full adiabatic Born-Oppenheimer basis  $\langle n | \langle nv |$  is used, where  $n$  and  $v$  denote the electronic and vibrational quantum numbers, respectively. For a multimode system  $v$  describes the whole set of vibrational quantum numbers. Under these assumptions the  $e$ -ph interaction, which is considered up to the second order, is based on the different potential surfaces in respect to the electronic excited and ground state. The linear  $e$ -ph interaction describes displaced oscillators and the quadratic terms include general mode mixing, frequency shifts, and additional equilibrium shifts due to electronic excitation. The potential surfaces are therefore arbitrary harmonic surfaces, but we neglect in our discussion the Duschinsky rotation, which describes mode mixing effects.

Non-Condon terms are regarded up to the first order. The usual assumption made in time-dependent theories of a constant linewidth also is assumed here to account for the lifetime for each of the vibrational levels in the electronic states. As we have performed all our experiments at about  $T=15$  K we use the  $T=0$  K approximation, which, however, is not a necessary condition for the theory.<sup>9</sup>

The time-correlator formulation for the optical absorp-

tion  $\alpha_j(\omega_L)$  in the dipole approximation at frequency  $\omega_L$  and light polarization  $j$  with lifetime broadening  $\gamma_e$  for the electronic excited level  $e$  and Lorentzian line shape is given by<sup>9</sup>

$$\alpha_j(\omega_L) = \sum_e \alpha_{j,e}(\omega_L), \quad (1)$$

where

$$\alpha_{j,e}(\omega_L) = B \hbar^{-1} (M_j^{eg}(\mathbf{0}))^2 \omega_L \times \text{Re} \left\{ \int_0^\infty dt \exp[it(\omega_L + i\gamma_e)] \eta_e(t) \right\}. \quad (2)$$

$M_j^{eg}(\mathbf{0})$  is the electronic dipole transition moment for  $j$  polarization from the ground level ( $g$ ) at an electronic excited level ( $e$ ) for the atomic equilibrium configuration ( $\mathbf{0}$ ) of the ground state,  $\eta_e(t)$  is the absorption correlator for the electronic excited level, and  $B$  is a frequency independent constant. Using the expressions given in Ref. 9 one can easily derive the  $T=0$  K approximation for the absorption correlator, which depends on the following:  $\omega_{eg}$  the effective electronic 0-0 transition frequency,  $\omega_{g,f}$  the ground ( $g$ ) state frequency of the normal mode  $f$ ,  $\omega_{e,f}$  the excited ( $e$ ) state frequency of the normal mode  $f$  (frequency shifted oscillators),  $\xi_{e,f}$  the dimensionless linear  $e$ -ph coupling constant (displaced oscillators), and  $m_{e,f}^j$  the linear non-Condon coupling constant (vibronic coupling).

### IV. RESULTS AND DISCUSSION

In Fig. 4 we show the polarized ( $E||z$ ) low-temperature absorption spectrum. The two symmetry allowed elec-

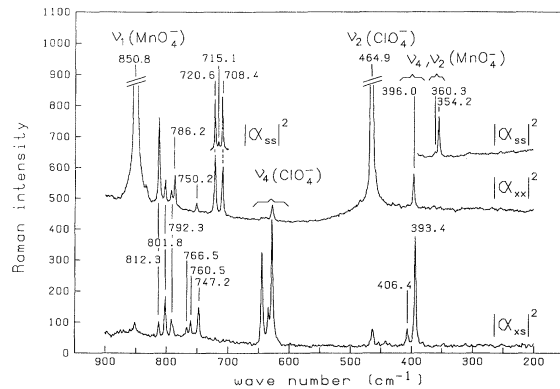


FIG. 2. Polarized resonance Raman spectra of a  $\text{KClO}_4$  single-crystal doped with  $\text{MnO}_4^-$  ions at  $T=15$  K between 200 and  $900 \text{ cm}^{-1}$ .  $\lambda_0=514.5 \text{ nm}$ .

TABLE III. Observed and calculated overtone and combination bands in the Raman spectra of the  $\text{MnO}_4^-$  ion doped in a  $\text{KClO}_4$  crystal at low temperature. Values are given in  $\text{cm}^{-1}$ .

Observed	Calculated	Difference
812.3	$2 \times 406.4 = 812.8$	-0.5
801.8	$406.4 + 396.0 = 802.4$	-0.6
792.3	$2 \times 396.0 = 792.0$	+0.3
786.2	$2 \times 393.4 = 786.8$	-0.6
766.5	$406.4 + 360.3 = 766.7$	-0.2
760.5	$406.4 + 354.2 = 760.6$	-0.1
750.2	$396.0 + 354.2 = 750.2$	$\pm 0.0$
747.2	$393.4 + 354.2 = 747.6$	-0.4
720.6	$2 \times 360.3 = 720.6$	$\pm 0.0$
715.1	$360.3 + 354.2 = 714.5$	+0.6
708.4	$2 \times 354.2 = 708.4$	$\pm 0.0$

TABLE IV. Symmetry and wave number positions of the site split  $\nu_2$  and  $\nu_4$   $\text{MnO}_4^-$  internal vibrations.

Wave number position:	406.4	396.0	393.4	360.3	354.2
Site symmetry:	$A'$	$A'$	$A''$	$A''$	$A'$
Free ion:	$\nu_4$			$\nu_2$	

tronic 0-0 transitions,  $A'(1) \leftarrow A'$  with  $18\,049\text{ cm}^{-1}$  and  $A'(2) \leftarrow A'$  with  $18\,081\text{ cm}^{-1}$ , are partially resolved in the absorption spectrum as indicated. According to the model presented above we have to deal with a maximum of four parameters in order to describe a single vibronic transition. These parameters are the vibrational ground frequency  $\omega_{g,f}$ , the excited vibrational frequency  $\omega_{e,f}$ , the dimensionless linear  $e$ -ph coupling constant  $\xi_{e,f}$ , and the non-Condon coupling constant  $m_{e,f}^x$ . In the following, we reduce the set of parameters by making use of symmetry arguments and of experimental results. The electronic ground state is fully symmetric ( $A'$ ) and in the polarization measurement with  $E \parallel x$  we can detect the  $A'$  components of the site split  ${}^1T_2$  level (see Fig. 4). Transitions to the  $A''$  level at  $18\,043\text{ cm}^{-1}$  would be symmetry allowed in this polarization in combination with an additional  $A''$  phonon. However, this is not confirmed by the absorption spectrum.

To describe the vibronic structure of the absorption spectrum we take only the symmetry allowed  $A'$  vibrations into consideration whose potential can have an

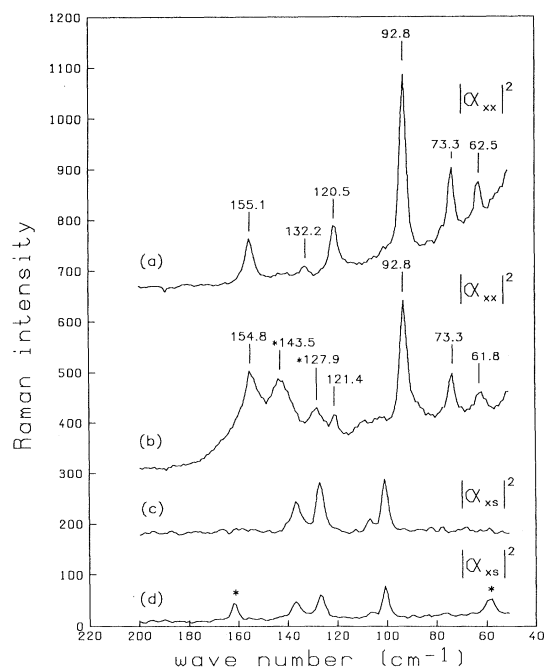


FIG. 3. Low-frequency Raman spectra of a  $\text{KClO}_4$  single-crystal, spectrum (a) and (c), at  $T = 15\text{ K}$  and the corresponding spectra, (b) and (d), of a  $\text{KClO}_4$  single crystal doped with  $\text{MnO}_4^-$  ions. The \* sign in spectrum (b) and (d) indicates non-localized Raman lines, whereby this sign denotes normal vibrations with  $A'$  symmetry of the  $\text{MnO}_4^-$  ion in spectrum (b) according to Table II.  $\lambda_0 = 514.5\text{ nm}$ .

equilibrium shift in the electronic excited state as compared to the ground state. Instead, the nontotally symmetric modes would break the symmetry in the electronic excited state. From the Raman spectra we derive the wave-number positions  $\omega_{g,f}$  of the normal modes in the electronic ground state. The  $A'-\nu_1$  frequency of the permanganate ion in two different electronic excited levels can be taken from the absorption spectrum. We find that within the accuracy of the measurement this value does not differ for the two electronic excited levels, which both have closely lying vibronic progressions which are responsible for the main structure.

A second significant structure in the low-temperature absorption (Fig. 4) is caused by an additional internal vibration of the permanganate ion (progression made up of the lower intense absorption bands). The frequency for this band at about  $300\text{ cm}^{-1}$  is independent of the two electronic excited states similarly as for the  $\nu_1$  mode. However, we are not certain which of the ground-state frequencies is involved in the absorption. The Raman spectra reveal that there exist three normal vibrations with  $A'$  symmetry which all have similar frequencies in the electronic ground state. There are two modes of  $A'$  symmetry resulting from the site split threefold degenerate  $\nu_4$  normal mode of the free ion and one mode of  $A'$  symmetry caused by the twofold degenerate  $\nu_2$  normal mode. The frequency ratio of the mode in the ground state and the one in the excited state ( $\omega_{g,f}/\omega_{e,f}$ ) is for the first set about 1.33 and for the second possibility about 1.17. The latter value is more reasonable. A final decision can only be made if the excited state frequencies are measured directly, e.g., by coherent anti-Stokes Raman spectroscopy. This could be performed using a preceding laser pulse to bring the permanganate ion into the excited electronic state and by a succeeding CARS experiment to localize the vibrational levels.

In the first model, to describe the low-temperature x-polarized absorption spectrum of the permanganate ion, we use the  $A'$  ground-state vibrations at  $\omega_{g,1} = 850.8\text{ cm}^{-1}$  and  $\omega_{g,2} = 354.2\text{ cm}^{-1}$ , and the two  $A'$  electronic excited levels at  $18\,049$  and  $18\,081\text{ cm}^{-1}$ . We also make use of the Condon approximation. With these values we

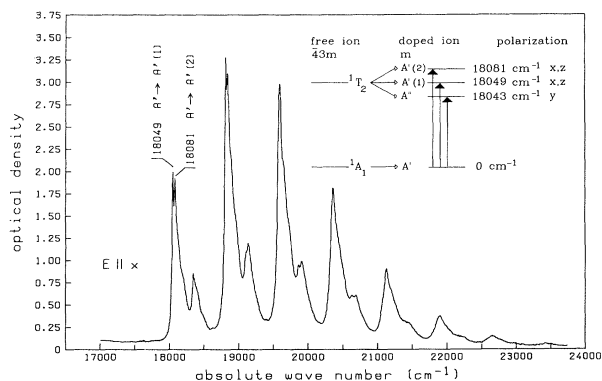


FIG. 4. Polarized absorption spectrum at  $T = 15\text{ K}$ . Also, the electronic level scheme with the corresponding site symmetry selection rules is given as an insert.

calculate the optical absorption  $\alpha_x$  as a function of the frequency  $\omega_L$  according to Eqs. (1) and (2). A damping constant of  $\gamma_e = \gamma_{A'(1)} = \gamma_{A'(2)} = 21 \text{ cm}^{-1}$  has been used for this purpose. The result is given in spectrum (a) of Fig. 5, together with the experimental spectrum (b) for comparison. Higher values for  $\gamma_e$  would cause too broad bands with loss of the vibronic structure caused by the site split  ${}^1T_2$  level of the permanganate ion. As can be seen, the intensity distribution of the two progressions as well as the steep shapes of the bands of the  $A'-\nu_1$  progression on the low-frequency side of each band are fairly well reproduced. However we note a high discrepancy as far as the band shape on the high-frequency side of each band is concerned. All bands show in fact a remarkable asymmetry.

In the next step, we have tried to correct this asymmetry by inclusion of low-frequency vibrations, i.e., localized modes of the permanganate ion, with  $A'$  symmetry and  $A_g$  phonons of the host lattice which are symmetry allowed. As they are fully symmetric they can have an equilibrium shift without destroying the local symmetry of the impurity centers under electronic excitation. These modes are shown above in the  $|\alpha_{xx}|^2$  spectra [see Figs. 3(a) and 3(b)]. In order not to increase the number of parameters needed for a theoretical simulation of the absorption spectrum, several additional assumptions were made: the frequency shifts of the low-frequency modes in the electronic excited levels were neglected and the non-Condon coupling was only allowed for the  $A'-\nu_1$  and  $A'-\nu_2$  modes of the permanganate ions.

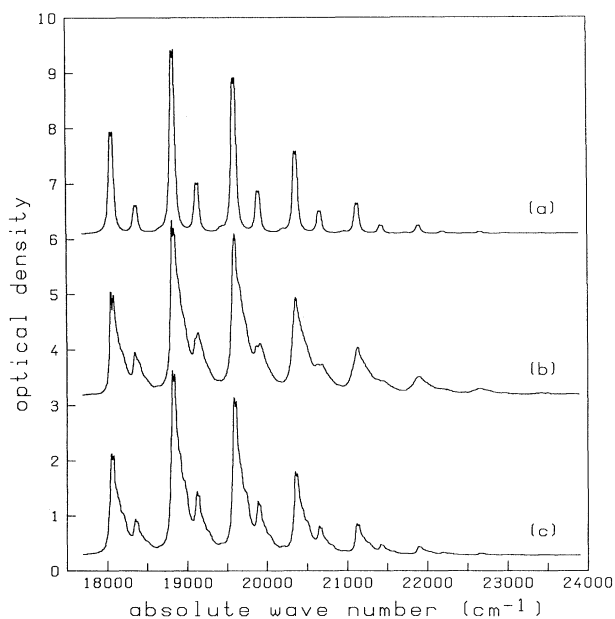


FIG. 5. (a) Calculated low-temperature absorption spectrum of the permanganate ion using a simple two vibrational mode  $\text{MnO}_4^-$  model. (b) Experimentally observed spectrum for comparison. For further details see text. (c) Calculated low-temperature absorption spectrum using an improved model where additional low-frequency modes were included. See Table V for parameters. All spectra were plotted with an offset.

The result of the best fit as compared to the experiment is displayed in Fig. 5, spectrum (c). A much better agreement with the experiment has been achieved now; particularly, the asymmetries of the absorption bands are well reproduced. The model parameters used for this simulation are given in Table V. We found that the non-Condon terms do not contribute appreciably. For the numerical calculation we used a program which allows to vary an arbitrary set of parameters, i.e., the number of modes and different combinations of normal mode parameters. We finally optimize the chosen parameter set by a least square fit. The time-correlator formulation for the optical absorption is very advantageous for the calculation of the absorption spectrum because of very low computational time. As an example, we need only one minute of computational time on a PC 80486 to calculate the complete spectrum with inclusion of nine vibrational modes and two electronic excited states and with a resolution of  $2.5 \text{ cm}^{-1}$  by using fast Fourier transformation according to Eqs. (1) and (2). The parameters which were optimized during the simulation procedure were the nine dimensionless linear  $e$ -ph coupling constants  $\xi_{e,f}$ , which were assumed to be independent on the electronic excited levels and the four non-Condon coupling constants  $m_{e,f}^x$  for the two internal modes of the permanganate ion. Altogether we have used the 9+4 already mentioned parameters plus the ratio of the two electronic dipole transition moments  $M_x^{A'(1)g}/M_x^{A'(2)g}$  as an additional parameter, for this nine-mode two-electronic excited level system. The calculated spectrum has been normalized to the 0-0 transitions which makes an additional scaling factor during the fit procedure unnecessary.

We like to state that the observed symmetry allowed modes in the  $|\alpha_{xx}|^2$  Raman spectra [3(a) and 3(b)] as displayed in Fig. 3 may not be complete and that strictly speaking the  $\mathbf{k}=0$  selection rule is no more valid for impurity centers. For example, phonons of the continuum of the acoustical branch may also contribute to the absorption spectrum. However, we found that the chosen set of low-frequency Raman modes is sufficient to explain the asymmetry of the bands in the absorption spectrum. The model parameters for the internal vibrations of the permanganate ion (high-frequency modes) are nearly constant when using different low-frequency modes. A restriction to only one low-frequency mode as it was done in Ref. 14 is a too crude approximation. A significant larger damping constant  $\gamma_e$  would have to be used then for the simulation with the consequence of nontolerable disagreement with the observed absorption spectrum.

The influence of eventual inhomogeneous line broadening seems to be negligible. If there are any inhomogeneous line broadening effects present in the electronic excited states, e.g., due to different sites of the molecules one has to calculate the convolution integral of the distribution function with the pure absorption spectrum in the frequency domain. This can easily be done by using the convolution theorem when calculating the absorption spectrum according to Eqs. (1) and (2) in the time domain.<sup>16,17</sup> Consideration of a Gaussian broadening in the simulation of the absorption spectrum of the permanganate ion has not improved the agreement with the ex-

TABLE V. Parameters for the simulation of the absorption spectrum of the permanganate ion. The model parameters were obtained from the experiments and the fit parameters were optimized during the numerical simulation of the absorption spectrum. For the simulation we used two  $\text{MnO}_4^-$  internal vibrations and additional seven low-frequency modes with two electronic excited levels. The frequencies of the modes are given in  $\text{cm}^{-1}$ .

Model parameters	$\text{MnO}_4^-$ modes				Low-frequency modes				
$\omega_{g,f}$	850.8	354.2	62.2	73.3	92.8	121.0	127.9	143.5	155.0
$\omega_{A'(1),f} = \omega_{A'(2),f}$	767.0	300.0	62.2	73.3	92.8	121.0	127.9	143.5	155.0
Fit parameters	$\text{MnO}_4^-$ modes				Low-frequency modes				
$\xi_{A'(1),f} = \xi_{A'(2),f}$	1.07	0.37	0.44	0.46	0.19	0.13	0.25	0.20	0.32
$m_{A'(1),f}^x = m_{A'(2),f}^x$	0.00	0.00			Not taken into account				
Ratio of the two electronic dipole transition moments ( $M_x^{A'(1)g}/M_x^{A'(2)g}$ )=1.2									

perimental spectrum. In case of a Lorentzian distribution function the convolution integral in the frequency domain yields to an expression where the homogeneous linewidth is substituted by only the sum of the homogeneous and the inhomogeneous contribution.<sup>18</sup> Without making any special assumptions the absorption spectrum is therefore not sensitive to a Lorentzian distribution function, but as it was shown in Ref. 18 the resonance Raman profile is influenced by an inhomogeneous Lorentzian distribution function. Resonance Raman profiles are therefore sensitive to this kind of line broadening. Khodadoost *et al.*<sup>17</sup> have discussed the  $A'-\nu_1$  Raman excitation profile of the permanganate ion doped in potassium perchlorate by using the transform theory. Their results are consistent with our simulation. They found that the inhomogeneous broadening does not significantly influence the excitation profile of the  $A'-\nu_1$  mode and its first two overtones.

So far we have restricted our discussion only to normal modes of the permanganate ion which have a significant influence in the absorption spectrum. Next we show the influence of other modes. As an example, we chose the site split  $\nu_3$  vibration of the permanganate ion. This degenerate vibration splits into  $2A' + 1A''$  components due to  $m(C_s)$  site symmetry. In principle, both  $A'$  modes are allowed by symmetry to appear in the absorption spectrum, but we restrict our discussion here to only one mode and we suppose that its frequency in the electronic ground state is about  $\omega_{g,3} = 920 \text{ cm}^{-1}$ . The exact value of this frequency is not of importance in contrast to  $\omega_{e,3}$ , the frequency in the electronic excited states, which we again suppose to be independent of the two electronic excited levels [ $A'(1)$  and  $A'(2)$ ]. A frequency ratio ( $\omega_{g,f}/\omega_{e,f}$ ) of about 1.2 seems to be a realistic value, which results in  $\omega_{e,3}$  to be  $770 \text{ cm}^{-1}$ . If the dimensionless linear  $e$ -ph coupling constant  $\xi_{e,3}$  of this mode is unequal to zero, this mode can show a progression. Note, however, that this progression coincides in frequency with the progression of the  $A'-\nu_1$  mode and contributes apparently to the observed intensity of the  $A'-\nu_1$  progression. To verify this effect we refer to Fig. 6. Spectrum (a) of this figure again shows the best fit as given above in Fig. 5, spectrum (c), where we have used the  $A'-\nu_1$  and the  $A'-\nu_2$  per-

ganate vibrations and the low-frequency modes for the calculation of the absorption spectrum. In the next step we calculate the absorption spectrum by using the  $A'-\nu_1$ ,  $A'-\nu_2$  and additionally the  $A'-\nu_3$  permanganate modes, whereby we used the parameter set of spectrum (a) and for the additional  $A'-\nu_3$  mode the following parameters:  $\omega_{g,3} = 920 \text{ cm}^{-1}$ ,  $\omega_{e,3} = 770 \text{ cm}^{-1}$ , and  $\xi_{e,3} = 0.27$ . Instead of showing the resulting calculated absorption spectrum, we display in Fig. 6(b) directly its difference to the spectrum displayed in Fig. 6(a). Note that we have normalized all spectra for each single simulation to the 0-0 electronic transitions. Curve 6(b) therefore gives the mentioned apparent intensity increase for the  $A'-\nu_1$  progression. In the last step of our model consideration we start from the calculated absorption spectrum which includes the  $A'-\nu_3$  mode and allow the value of the non-Condon coupling of the  $A'-\nu_1$  mode to be unequal to zero. For the selected values of  $m_{A'(1),1}^x = m_{A'(2),1}^x = m_{e,1}^x = -0.058$  we have again generated the difference to spectrum (a). The result is shown as spectrum (c) in Fig. 6,

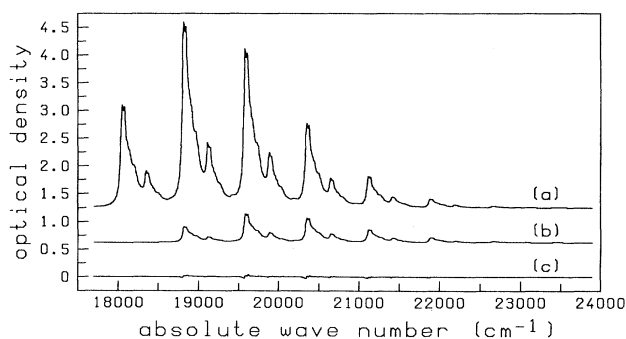


FIG. 6. Simulations of the low-temperature absorption spectrum of the permanganate ion in a  $\text{KClO}_4$  single crystal. (a) Same as spectrum (c) in Fig. 5. (b) Difference spectrum of a spectrum with inclusion of an additional  $A'-\nu_3$  mode with the following parameters:  $\omega_{g,3} = 920 \text{ cm}^{-1}$ ,  $\omega_{e,3} = 770 \text{ cm}^{-1}$ ,  $\xi_{e,3} = 0.27$ , and spectrum (a). (c) Same as (b) except for inclusion of a non-Condon coupling of the  $A'-\nu_1$  mode with  $m_{e,1} = -0.058$ . Curves (a) and (b) were plotted by using an offset.

which for the displayed frequency range is nearly close to zero. Hence, we have found two parameter sets which produce nearly identical simulated spectra.

The question remains if there are any non-Condon effects in our system. The answer cannot be given directly via the simulation of the absorption spectrum. Therefore, we need a method which is mode selective, as is the transform theory. Experimentally, we can derive the information needed by measuring the excitation profile of the mode of interest.

We will now estimate how accurate the parameters of the high-frequency modes can be derived by comparing the different parameter sets needed for the description of the absorption spectrum. As an example, we discuss the case where the  $A'-\nu_3$  mode is taken into account within the Condon model. To achieve agreement with the experiment we vary the dimensionless linear  $e$ -ph constant  $\xi_{e,1}$  and the  $A'-\nu_1$  mode. Within this procedure and by using different parameters we can estimate the relative error of the model parameter and achieve  $\xi_{e,1} = 1.07 \pm 0.08$ . It is therefore reasonable to discuss the physical significance in more detail for this selected parameter.

According to Refs. 17 and 19 the relation of the dimensionless linear  $e$ -ph coupling constant and the usual Franck-Condon factors in the absence of non-Condon coupling is given by the following expression:

$$\xi_{e,f}^2 = \frac{\omega_{e,f}^3 (\omega_{e,f} + \omega_{g,f})^2 |\langle e1_f | g0_f \rangle|^2}{4\omega_{e,f}^5 |\langle e0_f | g0_f \rangle|^2},$$

whereby the additional index  $f$  indicates that  $\langle nv_f |$  describes a single oscillator function of mode  $f$  in the electronic level  $n$ .

Using the recurrence relations of Manneback<sup>20</sup> one can serve

$$\xi_{e,f}^2 = \frac{\pi}{h} \Delta Q_{e,f}^2 \frac{\omega_{e,f}^4}{\omega_{g,f}^3},$$

where  $\Delta Q_{e,f}$  is the change of the equilibrium position of the normal coordinate in the electronic excited state relative to the ground state.<sup>21</sup> The  $\nu_1$  normal mode of the free permanganate ion ( $T_d$  symmetry) consists of purely Mn-O stretching.<sup>22</sup> The symmetry coordinate is then only proportional to the change in the bond length. According to Ref. 23 the change in the normal coordinate is given by  $\Delta Q = \sqrt{\mu} \Delta S$ , whereby  $\mu$  is the mass of the oxygen atom and  $\Delta S$  the change of the symmetry coordinate, which is related to the change in the bond length by  $\Delta S = 2\Delta_{\text{Mn-O}}$ . If one neglects the distortion in the geometry of the tetrahedral permanganate ion in the host lattice, one can use the given formulas to calculate the change in the equilibrium bond length. For the  $A'-\nu_1$  mode one obtains under these assumptions a value of  $4.6 \pm 0.4$  pm, whereby the error is approximated using limiting values of the dimensionless linear  $e$ -ph constant resulting from the calculation of the absorption spectrum. This value is in agreement with results reported by Clark and co-workers<sup>23,24</sup> which were derived from the resonance Raman excitation profile of the  $A'-\nu_1$  vibra-

tion. In the work reported, the experiments have been performed at room temperature and the theoretical description was such that only the  $A'-\nu_1$  mode was considered.

The equilibrium bond change mentioned above is relatively small compared to the Mn-O average bond length<sup>25</sup> of  $162.9 \pm 0.8$  pm obtained from x-ray experiments. In this work the experiments were done at  $T = 77$  K on pure potassium permanganate which is isomorph to potassium perchlorate with similar lattice constants.<sup>26,27</sup> The distortion of the permanganate tetrahedron due to the  $m$ -site symmetry lies within the error limit of the experiments. The theoretical description of the absorption spectrum with a common set of model parameters for the two electronic excited states results in a reasonable agreement between experiment and theory. As we have shown, the influence of non-Condon effects is not definitely due to the appearance of nonsignificant modes. The agreement between the experiment and theory for the spectral range between about 18 000 and 21 000  $\text{cm}^{-1}$  is quite good. However, for higher wave numbers ( $\bar{\nu} > 21 000 \text{ cm}^{-1}$ ) the values of the calculated optical density are smaller than detected experimentally. This is probably due to the fact that higher-order corrections, e.g., cubic  $e$ -ph coupling, which are not included in the theoretical model, become more and more important for higher wave numbers.

## V. SUMMARY AND CONCLUSION

Within the time-correlator formulation of the optical absorption we have described the low-temperature absorption spectrum of the permanganate ion doped in a potassium host crystal by using two internal permanganate vibrations and two electric excited levels. The linewidth was taken from the absorption spectrum under the condition that the electronic structure is resolvable. The asymmetry of the observed absorption bands could be described when additional low-frequency modes, extracted from the Raman spectra, were included in the simulation. We further discussed the simulated spectrum with inclusion of an additional  $A'-\nu_3$  permanganate vibration. We showed that several sets of parameters yield to nearly the same simulated absorption spectrum, leaving the question opened if non-Condon effects have to be considered for the calculation of the absorption spectrum.

Model parameters of significant modes, for example, the dimensionless linear  $e$ -ph constant of the  $A'-\nu_1$  mode, have been discussed in regard to their physical significance. For this parameter we have calculated the change in the Mn-O equilibrium bond length. The calculation of the absorption spectrum yields to the important result that the model parameters of the relevant normal modes are equal for both electronic excited levels. Therefore, it is not necessary to deconvolute the absorption spectrum when the transform theory is used for the description of the excited profile. Here, likewise in the presence of only one electronic excited state, the transform theory can be directly applied. Work on this regard is in progress, particularly to simulate observed CARS-

excitation profile for the  $A'-\nu_1$  permanganate vibration.<sup>10</sup>

In the case of no mode-mixing effects, the transform theory is mode selective. This is a big advantage, because it is then possible to derive more definite information on the influence of the non-Condon effect caused by the  $A'-\nu_1$  permanganate mode. The results of this discussion are given elsewhere.<sup>28</sup>

#### ACKNOWLEDGMENTS

We like to thank Professor J. B. Page for fruitful discussions. He suggested to use the time-correlator formulation for the description of the optical absorption. Financial support from the Fonds der Chemischen Industrie e.V. and the Deutsche Forschungsgemeinschaft (SFB 347, Projekt C-2) is acknowledged as well.

\* Author to whom correspondence should be addressed.

<sup>1</sup>D. L. Tonks and J. B. Page, *Chem. Phys. Lett.* **66**, 449 (1979).

<sup>2</sup>D. L. Tonks and J. B. Page, *Chem. Phys. Lett.* **79**, 247 (1981).

<sup>3</sup>D. L. Tonks and J. B. Page, *J. Chem. Phys.* **75**, 5694 (1981).

<sup>4</sup>D. L. Tonks and J. B. Page, *J. Chem. Phys.* **76**, 5820 (1982).

<sup>5</sup>C. K. Chan and J. B. Page, *J. Chem. Phys.* **79**, 5234 (1983).

<sup>6</sup>C. K. Chan and J. B. Page, *Chem. Phys. Lett.* **104**, 609 (1984).

<sup>7</sup>D. L. Tonks and J. B. Page, *J. Chem. Phys.* **88**, 738 (1988).

<sup>8</sup>H. M. Lu and J. B. Page, *J. Chem. Phys.* **88**, 3508 (1988).

<sup>9</sup>See, for example, J. B. Page, in *Light Scattering in Solids VI*, edited by M. Cardona and G. Güntherodt (Springer-Verlag, Berlin, 1991).

<sup>10</sup>M. Leuchs, A. Materny, D. Göttges, K. Schaschek, and W. Kiefer, *J. Raman Spectrosc.* **23**, 673 (1992).

<sup>11</sup>A. Materny, M. Leuchs, and W. Kiefer, *Il Nuovo Cimento* **14**, 989 (1992).

<sup>12</sup>W. Hayes and R. Loudon, *Scattering of Light by Crystals* (Wiley, New York, 1978).

<sup>13</sup>M. Tinkham, *Group Theory and Quantum Mechanics* (McGraw-Hill, New York, 1964).

<sup>14</sup>C. J. Ballhausen, *Theor. Chim. Acta.* **1**, 285 (1963).

<sup>15</sup>G. Turrell, *Infrared and Raman Spectra of Crystals* (Academic, London, 1972).

<sup>16</sup>C. K. Chan, J. B. Page, D. L. Tonks, O. Brafman, B. Khodadoost, and C. T. Walker, *J. Chem. Phys.* **82**, 4813 (1985).

<sup>17</sup>B. Khodadoost, S. A. Lee, J. B. Page, and R. C. Hanson, *Phys. Rev. B* **38**, 5288 (1988).

<sup>18</sup>R. A. Desiderio and B. S. Hudson, *Chem. Phys. Lett.* **61**, 445 (1979).

<sup>19</sup>O. Brafman, C. K. Chan, B. Khodadoost, J. B. Page, and C. T. Walker, *J. Chem. Phys.* **80**, 5406 (1984).

<sup>20</sup>C. Manneback, *Physica XVII*, 101 (1951).

<sup>21</sup>Tonks and Page have given a similar expression in Ref. 4. We have used the expressions given in Refs. 17 and 19. By using Manneback's recursion relations (Ref. 20 and Ref. 23), we are then able to express the change of the normal coordinate  $\Delta Q_{e,f}$  by the change of the symmetry coordinate  $\Delta S$ . We have chosen this way because of the factor of 2 mentioned in Ref. 23.

<sup>22</sup>G. Herzberg, *Molecular Spectra and Molecular Structure*, (Krieger, Malabar, FL, 1991), Vol. II.

<sup>23</sup>R. J. H. Clark and T. J. Dines, *Angew. Chem.* **98**, 131 (1986). This paper includes a remark of an error in the relation of symmetry coordinate  $\Delta S$  and the change in the bond length for tetrahedral molecules. This error is responsible for a mismatch of a factor of 2 in the result of the change of the equilibrium bond length in several papers (including Ref. 24) of this kind of molecules.

<sup>24</sup>R. J. H. Clark and B. Stewart, *J. Am. Chem. Soc.* **103**, 6593 (1981).

<sup>25</sup>G. J. Palenik, *Inorg. Chem.* **6**, 503 (1967).

<sup>26</sup>K.-H. Hellwege, *Zahlenwerte und Funktionen aus Naturwissenschaft und Technik*, Landolt Börnstein, New Series, Vol. 7, Group III, Part b2 (Springer-Verlag, Berlin, 1977).

<sup>27</sup>K.-H. Hellwege, *Zahlenwerte und Funktionen aus Naturwissenschaft und Technik*, Landolt Börnstein, New Series, Vol. 7, Group III, Part f (Springer-Verlag, Berlin, 1977).

<sup>28</sup>M. Leuchs and W. Kiefer, *J. Chem. Phys.* (to be published).